Characterization of the Capric and Lauric Acid Mixture with Additives as Thermal energy Storage Medium for Cooling Application

M. N. R. Dimaano[1] and T. Watanabe[2]

[1]Research Center for the Natural Sciences
University of Santo Tomas, España, Manila, 1008 Philippines

[2]Research Laboratory for the Nuclear Reactors
Tokyo Institute of Technology, 2-12-1 O-okayama, Meguro-ku
Tokyo 152-8550 Japan

The mixture of capric acid and lauric acid (C-L acid), with the respective mole composition of 65% and 35%, is a potential phase change material. It possesses the required desirable thermodynamic properties, higher energy density, reproducible melting and cooling behavior, no supercooling, non-toxic, non-corrosive, with definite melting temperature. However, its melting point of 18.0 ^{o}C is high for low temperature thermal energy storage. Compatibilities of the C-L acid in combination with some organic additives and their melting characteristics were initially determined using the DSC analysis. Different proportions of the mixture elucidated the temperature depression in the C-L acid system. Supplementary tests to evaluate the thermophysical and heat transfer characteristics of the C-L acid with pentadecane (CL:P) in different proportions were conducted. The heat transfer behavior and thermal storage performance were verified, subjecting each combination to a series of thermal processes.

INTRODUCTION

Air conditioners and refrigerators make daily living comfortable but they have also endangered life in this planet. Recognizing the implications of the ozone destroying refrigerants, nations throughout the world are triggered to search for alternatives to the current refrigeration and air conditioning technology. An available technology involves thermal energy storage that offers capital cost savings on premium fuels and cost effectiveness due to the reduction of energy wastage. It can even offer the best way to shift peak energy consumption to off peak periods with the advantage of cheap electric charges.

The latent heat storage technology employing the solid to liquid phase change is of particular interest in this study. It is capable of storing large amount of thermal energy in a small volume with lower energy loss and a reasonably small temperature swing [1]. On the basis of local availability and abundance in raw materials, fatty acids are considered as the main phase change materials (PCMs). The Philippines is a primary producer of coconut oil. Fatty acids like capric acid and lauric acid are derived from coconut oils. Out of 100g of coconut oil, 86g are fatty acid. Of this fatty acid, 50% is capric acid and 15% is lauric acid. A recent study showed that a mixture of 65% capric acid and 35% lauric acid, by mole composition (C-L acid), signified a latent heat of 148 kJ/kg and a melting point of 18.0 ^{o}C [2]. However, this melting point is considered high for thermal energy storage specifically for cooling. Possible lowering of melting temperature and improving the heat transfer characteristics had been previously investigated [3, 4].

Initial differential scanning calorimetry (DSC) analysis provided that pentadecane is capable of lowering the melting point of the C-L acid mixture to as low as 10.2 ^{o}C. The optimal C-L acid combination that melts at 7 to 10 ^{o}C with a substantial heat of fusion for cooling application has yet to be determined. This study considers the screening of additives to optimize the C-L acid mixture proposed for this temperature range.

This study is aimed at evaluating the thermal characteristics of the combinations of the C-L acid with these additives in different proportions employing the differential scanning calorimetry (DSC) analysis. The heat transfer and thermal storage performance of probable C-L acid combinations encapsulated in a vertical cylindrical heat exchanger are further elucidated subjecting them to a series of charging and discharging processes.

MATERIALS AND METHODS

Capric acid, lauric acid (both 98% purity), and pentadecane (99% purity) were manufactured by Tokyo Chemicals, Inc. The melting characteristics of the C-L acid with different additives were evaluated: caproic acid, eugenol, cineole, ethyl benzoate, and oleic acid. The selection of these additives were based on their low melting points, low vapor pressure, and non-aromatics avoiding carcinogens. Probable additives that lower melting points of compounds are manifested in chemical structures that have shorter carbon chain with more double bonds that effect temperature depression.

Caproic acid (99% purity), eugenol, and cineole were produced by Sigma Chemical Co.; ethyl benzoate (99+% purity) were manufactured by Aldrich Chemical Co., Inc.; and the oleic acid, from D & L Industries, Inc. Nine mole fractions (0.02, 0.04, 0.06, 0.08, 0.10, 0.20, 0.30, 0.40, & 0.50) of the additives were individually prepared and made homogeneous in the C-L acid base mixture of 65% capric acid and 35% lauric acid, by mole.

Prior analysis of the pure C-L acid system provided a melting point of 18.0 ^{o}C and a heat of fusion of 140.8 kJ/kg. The melting characteristics of the C-L acid with the corresponding additives were determined using a Mettler Toledo DSC821. Representative sample weights of 8-15 mg were taken in each mixture analysis and heating was controlled at a rate of 2.5 ^{o}C/min.

In order to consider the changing composition of a solution, the changes that occur with different volume concentrations has been utilized considering volume as the most easily visualized property for mixture evaluations. Additional examinations of the heat transfer behavior and thermal storage performance of C-L acid with pentadecane (CL:P) in different volume proportions (90:10, 70:30, and 50:50) were conducted. Each CL:P combination was subjected to a series of thermal processes. The radial and axial temperature distribution in the CL:P during charging and discharging were determined.

Thermal Storage Facility

A schematic of the experiment set-up employed to evaluate the latent heat storage performance of the CL:P combination as phase change material (PCM) for cooling application is shown in Figure 1. It consists of a storage capsule, cooler, heater, datalogger/converter, computer, rotameter, pumps and valves. The storage capsule is made up of a copper tube that is concentrically fixed in an annular acrylic cylinder. A PCM mass of 0.20 kg is encapsulated inside the copper tube while water as the heat transfer fluid flows continuously through the cylinder. Inlet water flows from the bottom of the cylinder at a rate of 1.67×10^{-5} m^3/s and controlled at 35 ^{o}C during charge (melting) process and at 2.2 ^{o}C during discharge (solidification) process. The cooler and heater provided the controlled temperature environment of the system.

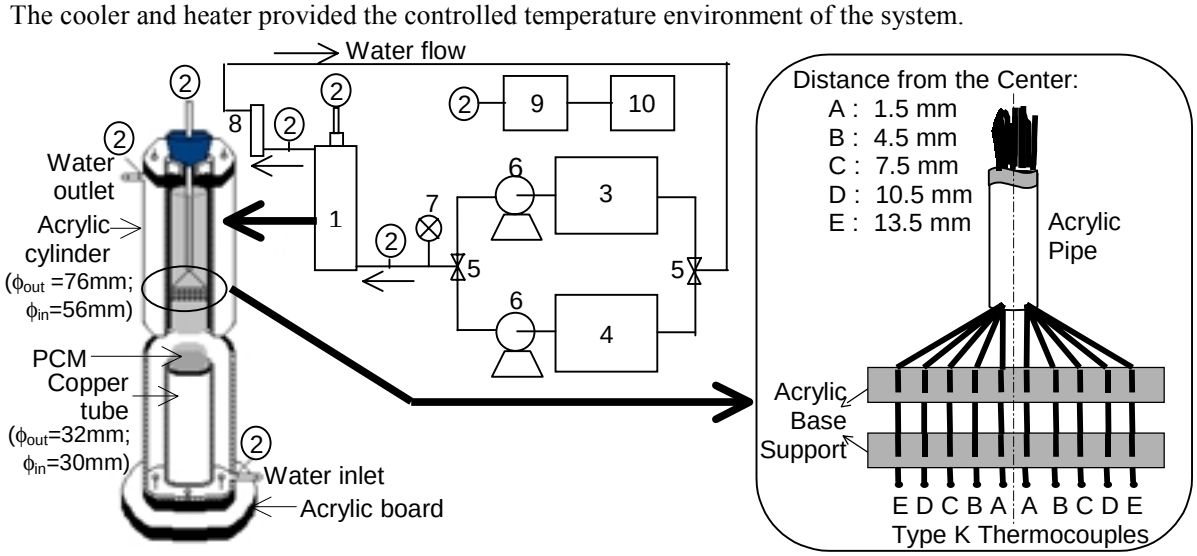

Figure 1 : A schematic diagram of the experiment set-up with the details of (1) the storage capsule. Inset shows the PCM probe fixture. Numbered labels are (2)-thermocouple/s; (3)-cooler; (4)-heater; (5)-gate valve; (6)-pump; (7)-water regulator; (8)-rotameter; (9)-data logger; (10)-computer.

The radial temperatures of the PCM are monitored throughout the process until they approach the temperature of the flowing water. The probe set-up used to determine the radial temperature distribution in the PCM is composed of 10 K-type thermocouples fixed at regular intervals of 3 mm (Figure 1 inset). The

axial (height) temperatures of the CL:P were likewise observed at different height positions for each experimental run at 0, 100, 200, and 300 mm from the base of the copper tube. All thermocouples were connected to a computer based data logger, recording data every 6 s of time interval. The whole system set-up was fiberglass insulated to ensure negligible heat loss.

DATA AND RESULTS

DSC Analysis

At least two thermal cycling tests were conducted per PCM sample. A PCM consists of C-L acid as the base system with caproic acid, cineole, ethyl benzoate, oleic acid, eugenol, and pentadecane, as additives. The melting behavior of the PCM is characterized by the heat of fusion, the peak temperature, and the melting width of the thermograms obtained from the DSC analysis. The differences in melting behavior of each sample are small enough to call the two cyclic tests per sample, DSC identical. After examining the DSC analysis of C-L acid with the component additives, a characteristic behavior in each system has been observed. The thermodynamic quantities vary with the composition of the system.

Temperature Depression

Intensive examination dealing with the thermodynamic quantities of the mixture requires the knowledge about the changes that occur when different amounts of any component are added to the mixture. An auxiliary analysis that is significant to this end is the determination of the melting temperature depression in the C-L acid mixture. The colligative property of a mixture is ideally demonstrated in very dilute solutions. That is why at lower concentration of additives, a more consistent decreasing trend follows a linear correlation between the temperature depression and the concentration of the mixture, as shown in Figure 2. A linear slope consistent in all of the PCMs with lower concentration of additives in the C-L acid, from 0 to 0.6 mole additive/kg C-L acid was established.

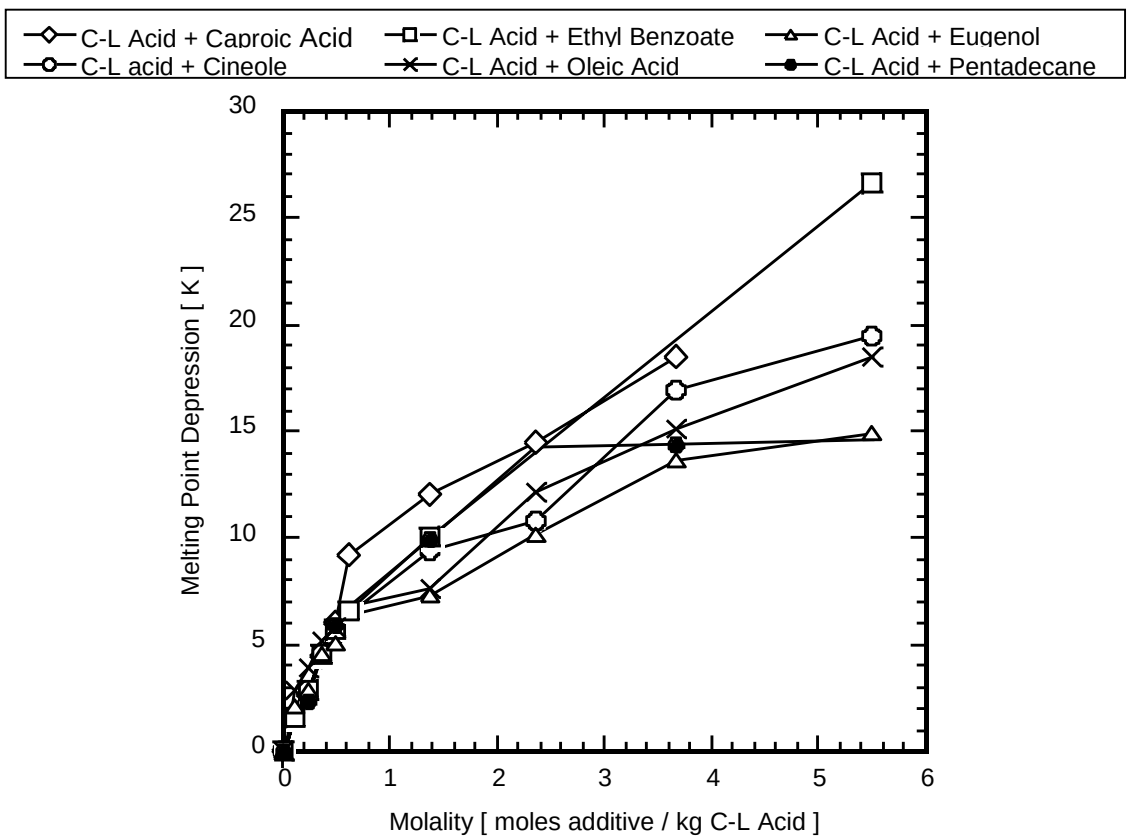

Figure 2 : Melting point depression of the C-L acid vs. the molality of the PCM mixture.

From this figure, the cryoscopic constant (K_f) was determined from the simple colligative equation.

$$\Delta T_{fus} = K_f \times m \tag{1}$$

in which

$$K_f = \frac{M_1 R T_{fus}^{*2}}{\Delta H_{fus}} \tag{2}$$

The slope obtained from equation (1) provided an average melting point depression constant of 10.6 K·kg/mol that conveys the distinctive characteristic of the C-L acid mixture. In lower concentrations of additives in the C-L acid, the latter is particularly the solvent while the additives are the solutes.

As the concentration of the additive is increased, the system becomes complex. The characteristic of the C-L acid is altered causing the deviation from its ideal condition. The real solvent cannot be distinctly identified due to the existence of more additive in the PCM mixture which at higher additive concentration makes the mixture a defined ternary system. Thus, the non-linearity between the temperature depression and the concentration of the mixture in increasing additive concentration, from 0.6 to 5.5 moles additive/kg C-L acid is markedly manifested in Figure 2. The temperatures of the mixtures drop variably, with the gradation depending on the additives' tendency to lower the melting point of the C-L acid. From the figure, it shows that the C-L acid + ethyl benzoate has the greatest temperature depression at higher concentrations. At the same concentration of about 1.4 mole additive/kg C-L acid, ethyl benzoate, pentadecane, and caproic acid provide the same temperature depression.

Since pentadecane has similar characteristics with the C-L acid in regard to chemical stability, recycleability, and chemical characteristics, its combination with the C-L acid is highlighted for further evaluation. Commensurate with the freezing point lowering is the inclination of the heat of fusion favoring the concentration of the component in the mixture. Unlike the C-L acid with other additives, two melting peaks were observed at higher concentrations of pentadecane as depicted in Table 1. An increasing trend with higher concentration of pentadecane is caused by the higher heat of fusion of pentadecane over the C-L acid. Interestingly, this increase in heat of fusion sets an advantage to energy storage system. Supplementary analysis is dealt with to substantiate what concentration of pentadecane is best for the C-L acid as evaluated from their effectiveness in the thermal energy storage for cooling application.

Effectiveness of the CL:P Combination

The relevant melting characteristics of C-L acid with pentadecane in different volume concentrations as obtained from the supplementary DSC analysis are presented in Table 1. Pentadecane in the C-L acid provided a melting range of 10.2 to 13.3 ^{o}C with a higher heat of fusion value of 142.2-157.8 kJ/kg compared with the pure C-L acid system. The shape of the thermal curves depicted in Table 1 provides the thermal history of the PCM. The DSC melting curves clearly show that the PCM is a blend of two components as indicated by the 2 peaks particularly at higher concentrations of both components in the mixture. With the thermophysical properties attributed to the PCM combinations provided in Table 2, their melting behavior is further evaluated subjecting the encapsulated PCM combination to a series of charging and discharging processes.

Table 1 : Melting band temperature limits and relevant thermal characteristics of C-L acid and pentadecane and their combinations obtained from DSC analysis.

% by Volume Ratio	Melting Band [^{o}C]		Melting Peak [^{o}C]	
C-L Acid : Pentadecane	Lower Limit	Upper Limit	CL Acid Side	Pentadecane Side
100 : 0	17.5	24.0	22.4	
90 : 10	9.0	21.4	19.9	
70 : 30	3.7	18.1	16.0	5.0
50 : 50	3.4	14.5	11.4	5.8
0 : 100	7.6	13.3		11.5

The radial temperature distribution representing the 70:30 CL:P combination at one height position during charging is shown in Figure 3. Since the initial temperature of the 70:30 CL:P combination is close to its lower melting band temperature limit, the radial temperatures during the initial stage of the melting process show an apparently flat distribution just before the onset of its phase transition. A slow rise in the temperature profile specifically in the inner radii is observed, subsequently due to the inward transfer of heat.

The temperature history in Figure 4 indicates the agreement of the DSC analysis to the thermal characteristics generated during the discharge process. The horizontal leveling of temperatures within the

melting band emerged twice conforming to the melting peaks generated from the DSC heating curves. Moreover, the temperature histories in both figures indicate that solidification takes longer time than melting.

Table 2 : Thermophysical properties of C-L acid and pentadecane.

	C-L Acid Mixture	90:10 CL:P	70:30 CL:P	50:50 CL:P	Pentadecane
Melting Point [°C]	18.0 †	13.3 †	11.3 †	10.2 †	9.6 †
Heat of Fusion [$kJ \cdot kg^{-1}$]	140.8 †	142.2 †	149.2 †	157.8†	168.0‖
Density (l) [$kg \cdot m^{-3}$]	894.9 ‡	883.2 †	858.0 †	827.8 †	727.2‖
Density (s) [$kg \cdot m^{-3}$]	900.0 ‡	891.3 †	872.7 †	850.4 †	776.1‖
Specific Heat (l) [$kJ \cdot kg^{-1} \cdot K^{-1}$]	2.24 †	2.42 †	2.57 †	2.89 †	3.53 †
Specific Heat (s) [$kJ \cdot kg^{-1} \cdot K^{-1}$]	1.97 †	2.08 †	2.27 †	2.44 †	3.08 †
Thermal Conductivity (l) [$W \cdot m^{-1} \cdot K^{-1}$]	0.139 ¶	-	-	-	0.15¶
Thermal Conductivity (s) [$W \cdot m^{-1} \cdot K^{-1}$]	0.143¶	-	-	-	0.182¶
Viscosity (l) [$Pa \cdot s$]	1.65×10^{-3}¶	-	-	-	2.62×10^{-3}¶

† - measured
‡ - (Mark *et al.*, 1978) [5]
¶ - (Humphries, 1977) [6]
‖ - (Lide, 1995) [7]

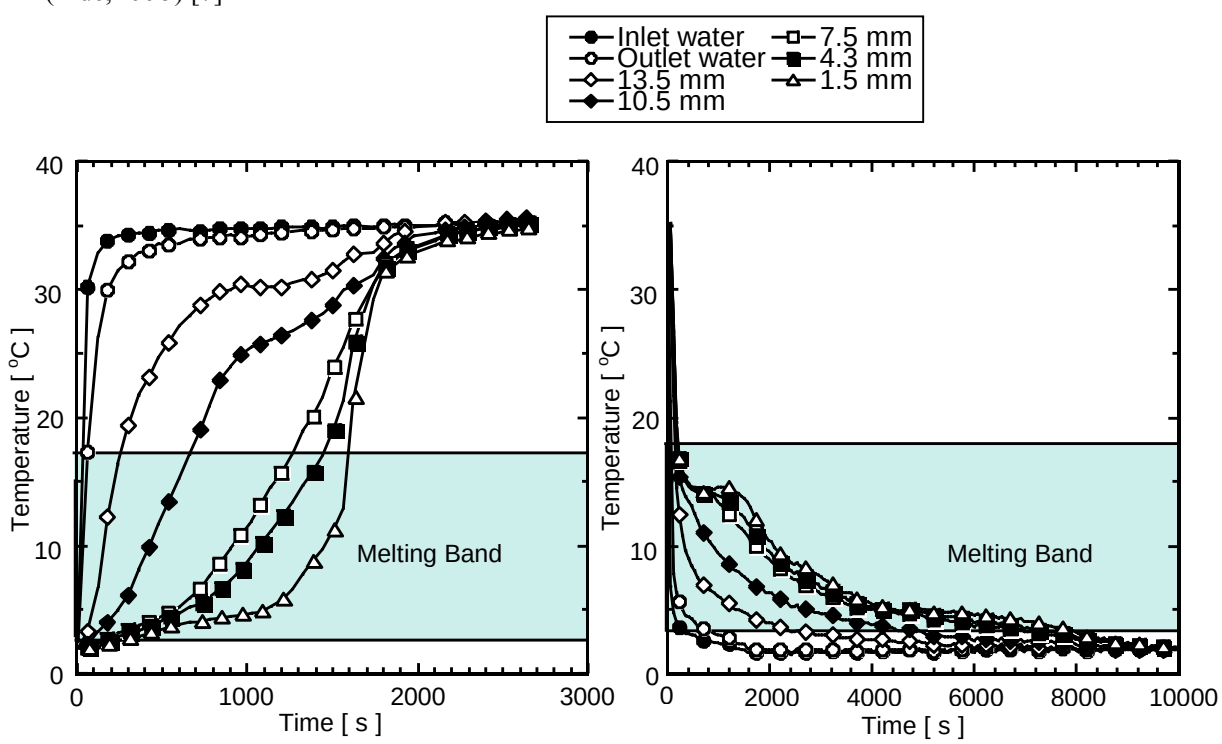

Figure 3 : Temperature history of 70:30 CL:P melting monitored at 100 mm probe height position with water maintained at an average temperature of 34.8 °C.

Figure 4 : Temperature history of 70:30 CL:P solidification monitored at 100 mm probe height position with water maintained at an average temperature of 2.3 °C.

The amount of heat charged and discharged by the CL:P during its melting and solidification were estimated from its radial temperature distribution at different height positions from the relations

$$dQ = \int_{Ts}^{T} 2\pi \, \rho_S \, Cp_S \, l \, r \, dr \, dT \, . \qquad (3)$$

$$dQ = \int_{Ts}^{Tm_1} 2\pi\, \rho_S\, Cp_S\, l\, r\, dr\, dT + \int_{Tm_1}^{T} 2\pi\, \rho_{ave}\, Cp_{ave}\, l\, r\, dr\, dT + \int_0^{\alpha} 2\pi\, \rho_{ave}\, L\, l\, r\, dr\, d\alpha \quad . \tag{4}$$

$$dQ = \int_{Ts}^{Tm_1} 2\pi\, \rho_S\, Cp_S\, l\, r\, dr\, dT + \int_{Tm_1}^{Tm_2} 2\pi\, \rho_{ave}\, Cp_{ave}\, l\, r\, dr\, dT + 2\pi\, \rho_{ave}\, L\, l\, r\, dr + \int_{Tm_2}^{T} 2\pi\, \rho_L\, Cp_L\, l\, r\, dr\, dT \tag{5}$$

and

$$Q = \int_0^R dQ \quad . \tag{6}$$

In storing heat, the latent heat energy storage uses some sensible heat storage below and above the CL:P melting temperatures, as well as the sensible heat and the latent heat drawn from its large melting band during phase transition. These are estimated from equations (3) to (5). The inner layer of either the liquid or solid phase during phase transition as latent heat is generated considers the melt/solid fraction (α) that grows as the CL:P gives up its heat of fusion. Equation (6) provides the total heat charged estimated throughout the process considering the radial direction from the center to the outermost radius of the CL:P inside the copper tube.

The thermal storage performance based on the total amount of heat stored during charging is shown in Figure 5. Consistent with the latent heats of pentadecane and the C-L acid as indicated in Table 2, pure pentadecane earlier supplied the highest charged energy followed by the 50:50 CL:P, 70:30 CL:P, 90:10 CL:P and finally the C-L acid system. The storage of energy depends on the thermodynamic properties of the PCM. The rate of charging is affected by the upper temperature limit of the melting band. Examine the increasing liquid sensible heat with higher concentration of pentadecane in the ternary blend. The upper melting band temperature limit affects the liquid sensible heat yield of the PCM mixtures specifically after phase transition, as shown in Table 3.

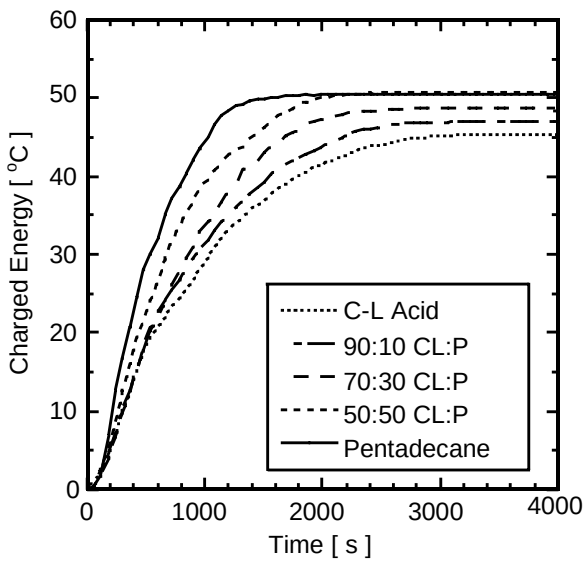

Figure 5 : Charged energies of the different CL:P combinations measured from the PCM radial temperature distribution.

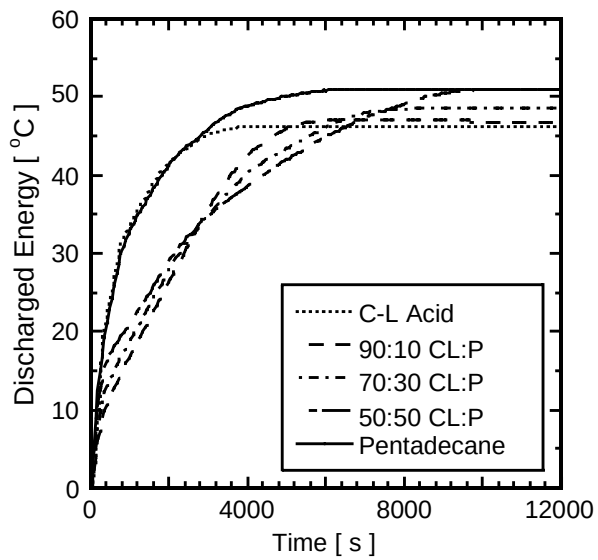

Figure 6 : Discharged energies of the different CL:P combinations measured from the PCM radial temperature distribution.

During the initial stage of the discharge process, pentadecane followed by the C-L acid readily released greater amount of energy. The 50:50 CL:P, 70:30 CL:P and the 90:10 CL:P combinations consequently follow this. Complications arise in the ternary blend during phase transition until about their melting peaks. The ternary blends proceed to discharge conversely, as indicated in Table 4. Although the higher concentrations of component additives in the ternary blend initially supply a greater amount of energy, they seem to hinder a faster discharge of energy. The presence of more composition of pentadecane in the mixture apparently causes slower discharge of energy as shown by the 50:50 CL:P in Figure 6. However, it ends up having similar values with pure pentadecane. Nevertheless, the discharge performance exhibited by the 90:10 presents a shorter solidification time with slightly improved energy storage ability.

Charging and Discharging Rates

A thermal energy load of short duration that is delivered with the small cooling equipment over a longer period of time is necessary in an efficient storage system for industrial and residential applications. The melting and solidification times play a vital role to ultimately measure the usefulness of the PCM. The melting time is estimated from the start of the charging process until the innermost radius of the PCM (refer to Figure 3) reaches the upper temperature limit of the melting band. The solidification time is determined from the start of the discharge process until the innermost radius of the PCM (refer to Figure 4) attains the lower temperature limit of the melting band. The melting times shown in Figure 7 show that melting proceeds from the highest to the lowest layer of the melting band affected by the control of natural convection governing on the upper layers of the PCM. More significantly, results depicted in the figure show the improvement in the performance of the C-L acid in terms of higher latent heat with lower melting point in relation to the melting time expended during the PCM charging.

Table 3 : Theoretical energy storage in the different stages of PCM charging.

	C-L Acid	90:10 CL:P	70:30 CL:P	50:50 CL:P	Pentadecane
Weight [kg]	0.21	0.20	0.20	0.20	0.18
Inlet water temperature [^oC]	35.0	34.9	35.3	34.9	34.9
Initial temperature of PCM [^oC]	2.1	2.3	2.2	3.0	2.8
Solid Sensible Heat [kJ]	6.4	2.9	0.7	0.2	2.7
Latent Heat [kJ]	29.6	29.0	29.5	30.4	30.2
Solid-Liquid Sensible Heat [kJ]	2.9	5.7	6.9	5.7	3.4
Liquid Sensible Heat [kJ]	5.2	6.6	7.7	11.2	13.9
Total Charged Energy [kJ]	44.1	44.2	45.8	47.5	50.2

Table 4 : Theoretical energy storage in the different stages of PCM discharging.

	C-L Acid	90:10 CL:P	70:30 CL:P	50:50 CL:P	Pentadecane
Weight [kg]	0.21	0.20	0.20	0.20	0.18
Inlet water temperature [^oC]	1.9	2.2	2.1	2.9	2.5
Initial temperature of PCM [^oC]	35.0	35.1	35.2	34.9	34.9
Liquid Sensible Heat [kJ]	5.2	6.7	8.7	11.2	13.7
Latent Heat [kJ]	29.6	29.0	29.5	30.4	30.2
Solid-Liquid Sensible Heat [kJ]	2.9	5.7	6.9	5.7	3.4
Solid Sensible Heat [kJ]	6.4	2.9	0.7	0.3	2.8
Total Discharged Energy [kJ]	44.1	44.3	45.8	47.6	50.1

Solidification takes longer time as it proceeds from the bottom to the upper layers along the vertical column of the PCM as shown in Figure 8. Noting the order of solidification times of the different PCMs, the lower temperature limit of the melting band shows a strong effect on solidification time. On the other hand, faster solidification is incurred at the highest layer implying that the PCM column exceeds its optimum height for an effective solidification. Longer PCM column height obstructs a suitable conduction to take place. Moreover, the pronouncement of the 90:10 CL:P combination as a better PCM blend that enhances the characteristics of the C-L acid mixture is established.

CONCLUSION

The DSC analysis of the PCM mixtures of C-L acid with some organic chemical additives elucidated the lowering of melting point of the C-L acid. A temperature depression constant of 10.6 K·kg/kmol provided the C-L acid 's distinctive characteristic. Furthermore, the storage assessment of the CL:P blends signifies the enhancement of the C-L acid mixture in the composition of 90:10 CL:P combination for cooling thermal energy storage system application.

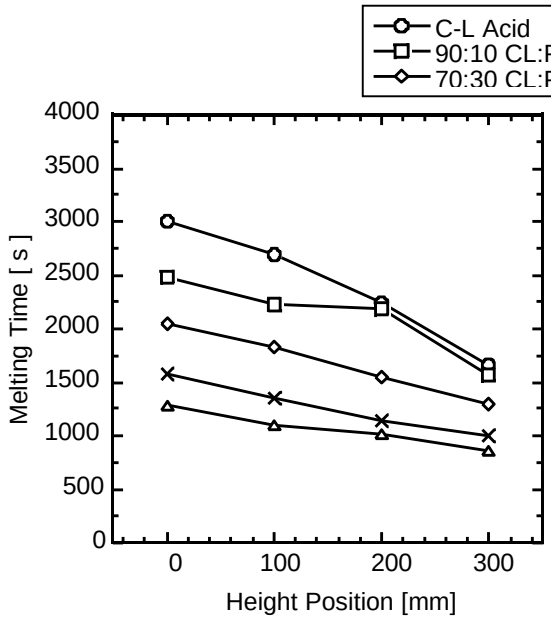

Figure 7 : Melting time of the different PCMs.

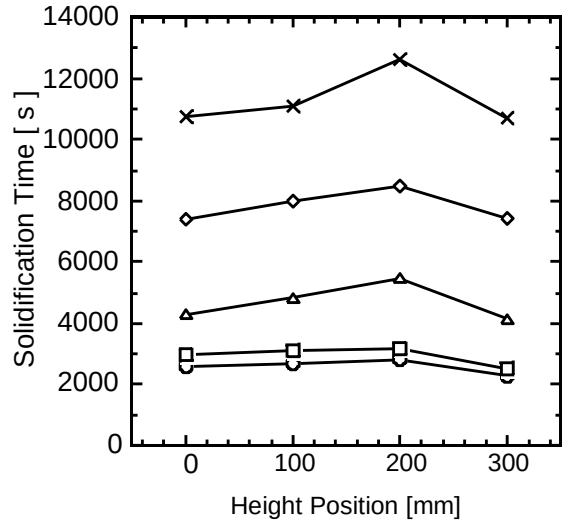

Figure 8 : Solidification time of the different PCMs.

NOMENCLATURE

Cp	specific heat of PCM [$kJ \cdot kg^{-1} \cdot K^{-1}$]
ΔH_{fus}	heat of fusion of C-L acid [$kJ \cdot mol^{-1}$]
l	height of the PCM in the capsule [m]
K_f	melting point depression constant [$K \cdot kg \cdot mol^{-1}$]
L	latent heat [$kJ \cdot kg^{-1}$]
M_1	molar mass of C-L acid [$kg \cdot mol^{-1}$]
m	molality of the PCM mixture [$K \cdot kg \cdot mol^{-1}$]
Q	total heat energy stored [kJ]
r	radial position [m]
R	universal gas constant [$kJ \cdot mol^{-1} \cdot K^{-1}$]
t	time [s]
T	PCM radial temperature [^oC]
T_{fus}*	melting point of C-L acid [^oC]
ΔT_{fus}	melting point depression [K] (melting point of C-L acid) – (melting point of the PCM mixture)
T_{m1}	lower melting band temperature [^oC]
T_{m2}	upper melting band temperature [^oC]
Ts	PCM start temperature [^oC]

Greek Symbols

α	melting or solidification fraction [–]
ρ	density of PCM [$kg \cdot m^{-3}$]

Subscripts

ave	averaged value from solid and liquid phases
S	solid phase of PCM
L	liquid phase of PCM

REFERENCES

1 Watanabe, T, Kikuchi, H. & Kanzawa A. (1993), 'Enhancement of Charging and Discharging Rates in a Latent Heat Storage System by Use of PCM with Different Melting Temperatures', *Heat Recovery Systems & CHP*, **13 (1)**, 57-66

2 Dimaano, M.N.R., & Escoto, A. (1998), 'Preliminary Assessment of a Mixture of Capric Acid and Lauric Acid for Low-Temperature Thermal Energy Storage', *Energy*, **23**, 421-427

3 Yoneda, N. & "Takanashi, S. (1978), 'Eutectic Mixtures for Solar Heat Storage', *Solar Energy*, **21**, 61-63

4 Aceves, S. M., Nakamura H., Reistad, G. M., & Martinez-Frias, J. (1998), 'Optimization of a Class of Latent Thermal Energy Storage Systems with Multiple Phase Change Materials', *Trans. ASME*, **120**, 14-19

5 Mark H. F., Othmer D. F., Overrberger C. G., & Seaborg G. T. (1985) *Kirk-Othmer Encyclopedia of Chemical Technology* **4**, 3rd ed., pp. 186-187. John Wiley and Sons, New York.

6 Humpries W. R. & Griggs E. I. (1977) A Design Handbook for Phase Change Thermal control and Energy Storage Devices. *NASA Technical Paper*, **1074**, 35.

7 Lide D. R. (1995) *CRC Handbook of Chemistry and Physics*, 76th ed. CRC Press, Boca Raton, Florida.